osteoclastic bone resorption plays a central role in the pathogenesis of osteoporosis, leading to fragility and fracture [24], with anti-resorptive drugs, represented by bisphosphonates, currently regarded as the first choice of treatment [4]. Recent studies using mouse genetics have identified regulators of osteoclast differentiation and function, among which receptor activator of NF-κB ligand (RANKL) has attracted considerable attention [2]. A humanized monoclonal antibody against RANKL, which has recently been shown to increase BMD by inhibiting bone resorption, is emerging as a new treatment option [14]. The discovery of the extracellular signals that control osteoclastogenesis is much anticipated and expected to provide an attractive target for the development of new diagnostic and therapeutic strategies.

In a search for new bone-resorbing cytokines using a *Xenopus* oocyte expression cloning technique, we have recently identified γ-glutamyltransferase (GGT or γ-GTP) as an osteoclastogenic factor, and demonstrated that recombinant human GGT as well as purified GGT from rat kidney stimulates bone resorption [16]. Further, during the course of our study examining the involvement of GGT in bone and joint diseases characterized by accelerated bone resorption, we unexpectedly found that GGT activity in urine, but not in serum, correlates with bone resorption. The present study was undertaken to determine whether GGT is a potential marker of bone resorption, using genetic mouse models as well as human subjects.

Materials and methods

Reagents

Alendronate sodium hydrate was purchased from Teijin Pharma Ltd. (Osaka, Japan). Human PTH (1–34) and M-CSF were kindly provided by Asahi Kasei Pharma (Tokyo, Japan) and Morinaga Milk Industry (Tokyo, Japan), respectively.

Animal experiments

Osteoprotegerin (OPG)-deficient male mice and BALB/cA mice were purchased from Clea Japan Inc. (Tokyo, Japan), and acclimated under standard laboratory conditions at 24±2°C and 50–60% humidity. The mice were allowed free access to tap water and commercial standard rodent chow (CE-2) containing 1.20% calcium, 1.08% phosphate and 240 IU/100 g vitamin D_3 (Clea Japan Inc., Japan). At the age of 9 weeks, OPG homozygous and heterozygous knockout mice (as control) were treated s.c. with vehicle (saline) or 1 mg/kg BW alendronate 5 times a week for 2 weeks, and urine was collected during the final 24 h. Blood samples were centrifuged to obtain the serum.

Eight-week-old female BALB/cA mice were infused with PTH at a rate of 4.3 pmol/h for 4 days. In brief, human PTH (1–34) was resolved in 2% L-cysteine solution, and loaded into Alzet osmotic minipumps. After equilibrated in saline at 37°C overnight, the pumps were implanted in a subcutaneous space on the back. Urine was collected during the final 24 h for biochemical analysis.

op/+ heterozygous mice were obtained from Jackson Laboratory (Bar Harbor, ME), and fed CE-2 powder chow (Clea Japan Inc., Japan). At the age of 5 weeks, *op/op* homozygous mice were treated i.p. with 5 μg M-CSF twice daily for 3 days, and urine and serum samples were collected before and after M-CSF treatment. Tibiae were removed for micro-CT scanning and tartrate-resistant acid phosphatase (TRAP) staining.

The animal experiments were carried out in accordance with the institutional ethical guidelines for animal care, and the experimental protocols were approved by the animal care committee of NCGG.

Subjects

Blood and spot urine samples were collected at 10:00–12:00 am from 10 patients with postmenopausal osteoporosis (67–83 years of age; average, 76.7), who visited the National Center for Geriatrics and Gerontology Hospital from April 2003 through August 2004, before and after alendronate treatment for measurement of blood GGT as well as urinary GGT and NTX. The diagnosis of osteoporosis was made based on the criteria recommended by the Japanese Society for Bone and Mineral Research [18], i.e., at least one non-traumatic vertebral fracture and a BMD lower than 80% of the young adult mean (YAM) or BMD lower than 70% of YAM without fracture.

Urine samples were also collected from 551 volunteer postmenopausal women (50–89 years of age; average, 66) at their regular health checkup for the measurement of GGT and deoxypyridinoline (DPD). The human studies were approved by the institutional review board, and written informed consent was obtained from all individuals.

Biochemical analysis

GGT activity and creatinine concentrations in the serum and urine were determined by using an autoanalyzer (model AU5232, Olympus) on the day following sample collection after storage at room temperature, since we found that GGT activity in the urine was stable for up to 1 week at room temperature or at 4°C but was lost after freezing at −20°C and subsequent thaw. Intra- and inter-assay variations for GGT were 0.58–1.77% and 0.29–1.78%, respectively. NTX and free DPD concentrations in the urine were measured using Osteomark [7] and Osteolinks-DPD (Sumitomo Seiyaku Biomedical Co., Ltd., Osaka, Japan) assay kits [20], respectively, and the values were corrected for creatinine. Intra- and inter-assay variations were 1.8–4.5% and 4.7–10.8% for NTX, and 1.4–7.4% and 4.2–6.4% for DPD, respectively. Leucine aminopeptidase, alkaline phosphatase, acid phosphatase and *N*-acetyl-β-D-glucosaminidase (NAG) in the urine were determined by using autoanalyzers (model AU5200 and AU600, Olympus).

Urinary GGT, creatinine and free DPD concentrations for the 551 volunteer women were measured by using "γ-GTP C-TestWako" (Wako Pure Chemical Industries, Ltd., Osaka, Japan) and "Determina-L CRE" (Kyowa Medex Co., Ltd., Tokyo, Japan) assay kits, respectively.

For fractionation of GGT activity, urine was collected from 6 healthy volunteers (3 females and 3 males; aged 29–35 years). After centrifugation at 17,000×*g* for 15 min, the supernatant was further centrifuged at 200,000×*g* for 3 h. GGT activity in the pellet and supernatant fractions after each centrifugation was measured using γ-GTP C-TestWako (Wako Pure Chemical Industries, Ltd., Osaka, Japan).

Bone analysis

For bone analysis, right tibiae were dissected and stored in 70% ethanol for micro-computed tomography scanning. Left tibiae were fixed in 4% paraformaldehyde, and TRAP staining was performed by a standard technique [17].

Micro-computed tomography scanning was performed on proximal tibias by using a μCT-40 (SCANCO Medical AZ, Bassersdorf, Switzerland) with a resolution of 12 μm, as described previously [8].

Statistical analysis

Data are expressed as the mean±SD. Changes in GGT and DPD or NTX excretion before and after alendronate treatment were analyzed by unpaired or paired Student's *t* test. The relation between GGT and DPD was assessed by Spearman rank order correlation analysis. $P<0.05$ was considered statistically significant.

Results

In order to determine if GGT is involved in bone diseases associated with accelerated bone resorption, we first assessed

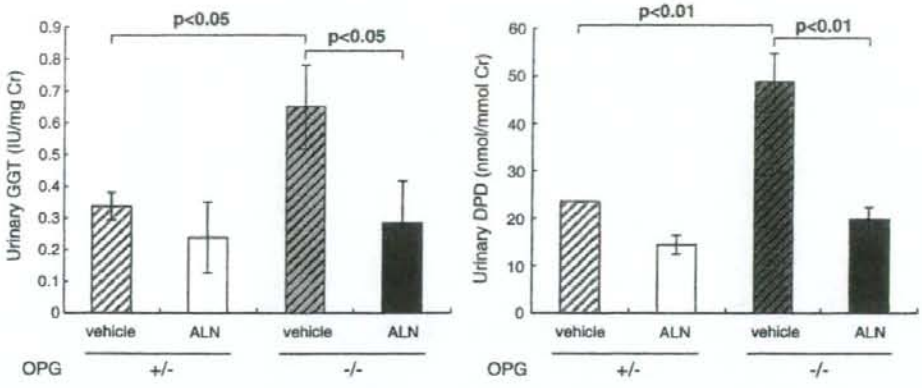

Fig. 1. Reduction in urinary GGT excretion after treatment of OPG-deficient mice with alendronate. Nine-week-old osteoprotegerin (OPG)-deficient male mice were treated s.c. with vehicle (saline) or 1 mg/kg BW alendronate (ALN) 5 times a week for 2 weeks, and urinary excretion of GGT (left) and DPD (right) was then determined. OPG heterozygous knockout mice served as the control. $n=3$ for vehicle groups and $n=7$ for treatment groups.

blood and urinary levels of GGT in a genetic model of osteoporosis, i.e., osteoprotegerin (OPG)-deficient mice [2]. OPG is a decoy receptor of RANKL, an essential cytokine for the formation of osteoclasts, and mice lacking OPG exhibit osteoporosis due to unopposed RANKL signaling and accelerated bone resorption [2]. Serum GGT activity in these mice was very low (less than 4 IU/l), compared with that in humans (normal range being 10–63 IU/l), and did not differ between OPG homozygous and heterozygous knockout mice or after treatment with alendronate, a selective inhibitor of bone resorption (data not shown). In contrast, as shown in Fig. 1, urinary excretion of GGT as well as of DPD was significantly increased in OPG homozygous knockout mice, compared with the levels of the control heterozygous mice. Treatment of OPG-deficient mice with alendronate resulted in a significant reduction in both urinary GGT and DPD excretion to the control levels found in the heterozygous mice. These findings suggest that urinary excretion of GGT, not serum levels, reflects the activity of bone resorption in the body.

Urinary excretion of leucine aminopeptidase (0.048±0.023 in WT vs. 0.065±0.021 U/mg Cr in OPG KO) and alkaline phosphatase (0.032±0.054 in WT vs. 0.021±0.015 IU/mg Cr in

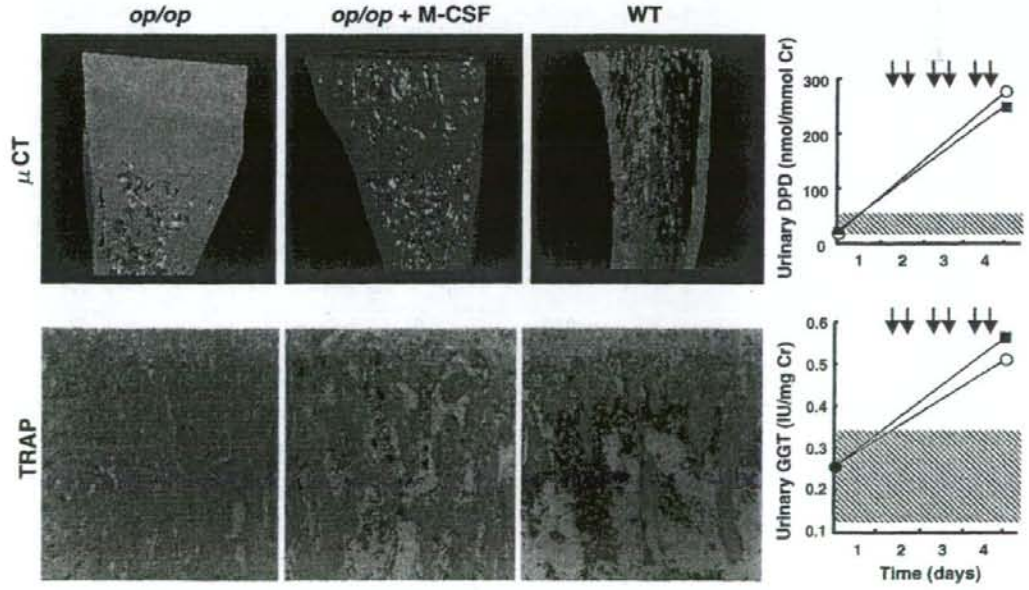

Fig. 2. Increase in urinary GGT excretion after osteoclast induction in *op/op* mice. Six-week-old osteopetrotic *op/op* female mice ($n=2$ each) were treated i.p. with 5 μg M-CSF twice daily for 3 days, and urinary excretion of DPD and GGT was then determined before and after injections. Age- and sex-matched wild-type mice served as the control as shown as the shaded area (mean±SD, $n=10$). Arrows indicate M-CSF injections. Representative micro-CT images and photomicrographs of TRAP staining of the proximal tibia are shown.

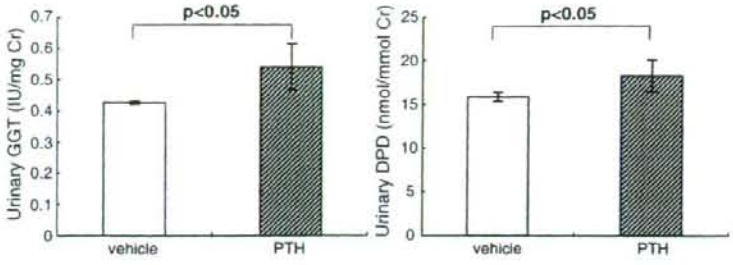

Fig. 3. Increase in urinary GGT excretion after constant PTH infusion. Eight-week-old female BALB/cA mice ($n=3$ each) were subjected to constant infusion of PTH (1–34) at a rate of 4.3 pmol/h for 4 days through Alzet osmotic minipumps, and urinary excretion of DPD and GGT was determined during the final 24 h. Age- and sex-matched mice with constant infusion of vehicle (2% L-cysteine) served as the control. Osteoclast surface and eroded surface per bone surface were markedly increased in the tibial metaphyses and lumbar vertebrae of PTH-infused mice.

OPG KO), enzymes located at the brush border membrane of renal tubules, did not differ significantly between wild-type and OPG knockout mice. Of lysosomal enzymes, urinary excretion of acid phosphatase did not differ (0.0030±0.0011 in WT vs. 0.0026±0.0015 IU/mg Cr in OPG KO), while that of *N*-acetyl-β-D-glucosaminidase (NAG) was significantly increased in OPG KO mice (0.066±0.028 vs. 0.193±0.074 IU/mg Cr, $p<0.01$). Thus, certain enzymes of proximal renal tubular cells including GGT may be excreted during elevated bone resorption.

We also employed a gain-of-function approach with another genetic model, osteopetrotic *op/op* mice, to examine whether urinary GGT excretion increases following the induction of osteoclasts with M-CSF injection. Fig. 2 shows representative micro-CT images (upper panel) and bone sections stained with TRAP activity (lower panel) at the proximal tibia. *op/op* mice at 6 weeks old exhibited typical osteopetrosis with very few osteoclasts, although osteoclasts appeared spontaneously with aging [17]. Administration of M-CSF twice daily for 3 days caused marked increases in bone marrow cavity and TRAP-positive osteoclasts (Fig. 2). Urinary DPD and GGT excretion both increased after M-CSF treatment (Fig. 2, right panel).

Continuous excess of PTH and PTH-related protein is associated with elevated bone resorption, as seen in patients with primary hyperparathyroidism and hypercalcemia of malignancy, respectively. As a model mimicking these conditions, we infused PTH (1–34) to mice constantly through osmotic minipumps. Histological examination on sections of tibial metaphyses and lumbar vertebrae revealed that osteoclast number and eroded surface per bone surface markedly increased following PTH infusion (data not shown). As shown in Fig. 3, constant infusion of PTH also increased urinary excretion of GGT significantly along with DPD. Collectively, our loss- and gain-of-function experiments using genetic and pharmacological models with excessive and deficient osteoclastic bone resorption, respectively, indicate that urinary GGT changes in parallel with DPD and reflects bone resorption activity in the body.

Based on these data, we analyzed urinary excretion of GGT in osteoporotic patients with elevated bone resorption. Urine samples were collected from 10 patients with postmenopausal osteoporosis (67–83 years of age; average, 76.7), before and after alendronate treatment. As shown in Fig. 4, urinary excretion of GGT decreased significantly along with NTX and DPD following treatment with alendronate. Serum GGT concentrations in these patients were within normal limits (10–63 IU/l) and did not change following treatment (data not shown).

In order to gain some insight into the form in which GGT exists in human urine, urine collected from healthy volunteers was fractionated by centrifugation, and the GGT activity in each fraction was determined. As shown in Table 1, when urine was centrifuged at 17,000×*g* (17 K) to remove cells and cell debris,

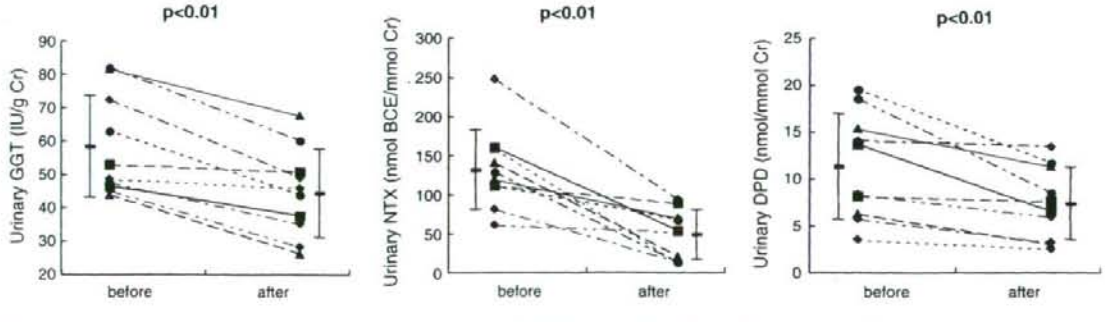

Fig. 4. Reduction in urinary GGT excretion after treatment of postmenopausal osteoporosis with alendronate. In 10 patients with postmenopausal osteoporosis (mean age: 76.7 years old), urinary excretion of GGT (left) decreased concomitantly with a reduction in urinary NTX (middle) and DPD (right) after treatment with alendronate (for 7 months on average). Individual data are shown with the mean±SD.

Table 1
Fractionation of urinary GGT activity

	Male				Female			
Urinary GGT	1	2	3	Mean	1	2	3	Mean
(IU/L)	32.7	37.0	63.6	44.4	45.3	30.8	14.6	30.2
17 K								
S	29.3	34.6	55.7	39.9	43.4	29.9	13.9	29.1
P	3.5	4.6	6.5	4.9	4.3	3.3	1.8	3.1
200 K								
S	6.5	6.3	9.5	7.4	5.0	6.3	3.5	4.9
P	23.7	26.9	47.0	32.5	36.5	28.9	13.3	26.2
% of P	72.5	72.7	73.9	73.2	80.6	93.8	91.1	86.8

Urine was collected from healthy volunteers (3 males and 3 females), and GGT activity in the whole urine was determined (top). After centrifugation at 17,000×*g* (17 K) and 200,000×*g* (200 K), GGT activity was determined in both supernatant (S) and pellet (P) fractions.

more than 90% of the total GGT activity in the urine was recovered in the supernatant fraction. When the 17 K supernatant was further subjected to centrifugation at 200,000×*g* (200 K), 73.2 to 86.8% of the total GGT activity was found in the pellet fraction, suggesting that GGT in human urine does not exist as a soluble form but rather is mostly associated with certain microstructures that sediment at 200 K.

Finally, to determine if urinary GGT can be used for screening individuals with elevated bone resorption in the general population, we assessed the urinary excretion of GGT and DPD in 551 volunteer postmenopausal women (50–89 years of age; average, 66) at their regular health checkup. As shown in Fig. 5A, there was a high correlation between urinary excretion of GGT and DPD in this population ($p<0.0001$). Of these 551 individuals, 113 had increased bone resorption, as judged from DPD values higher than 7.6 nM/mM Cr (17.0±15.0), the cut-off value for diagnosing elevated bone resorption recommended by the Japanese Society for Bone and Mineral Research. These individuals exhibited significantly elevated urinary excretion of GGT (85.7±95.0 IU/g Cr), compared with those that had normal DPD values (GGT: 22.0±12.0 IU/g Cr, DPD: 3.8±1.9 nM/mM Cr; Fig. 5B). When a cut-off value of 40 IU/g Cr was assigned for urinary GGT, the calculated sensitivity and specificity for discriminating those with elevated bone resorption, as determined by a DPD value higher than 7.6 nM/mM Cr, were 61% and 92%, respectively, and 75% and 79% for a GGT cut-off value of 30 IU/g Cr.

Discussion

GGT is an ectopeptidase that catalyzes the transfer of a γ-glutamyl moiety to an acceptor and plays a critical role in glutathione degradation and cysteine metabolism [11,23]. Mice deficient in GGT exhibit growth retardation, cataracts and severe osteoporosis, and die early at 10–18 weeks of age [12]. Osteopenia of GGT-deficient mice is due mainly to impaired bone formation, which is reversible by supplementation with *N*-acetylcysteine, suggesting that GGT plays an important physiological role in regulating bone formation through cysteine metabolism [10]. We have identified GGT as a bone-resorbing factor in the expression cloning of an osteoclastogenic activity contained in murine T lymphoma, which caused marked osteolysis in mice, and demonstrated that recombinant GGT at 100 IU/l, a level often seen in patients with excess alcohol intake or fatty liver, is indeed capable of stimulating osteoclastogenesis in bone marrow cultures [16]. Furthermore, the generation of transgenic mice overproducing GGT has revealed that excess GGT causes osteopenia due to accelerated bone resorption (Hiramatsu et al. manuscript submitted). Taken together, it is suggested that GGT levels should be maintained within a set physiological range and both deficiency and excess can lead to osteoporosis, but by distinct mechanisms, i.e., through suppressed bone formation and elevated bone resorption, respectively. Interestingly, a mutated GGT molecule devoid of enzyme activity is fully active in promoting osteoclast formation (Hiramatsu et al. manuscript submitted), suggesting that the osteoclastogenic function of GGT is dissociated from its enzyme activity, does not involve glutathione or cysteine metabolism, and may represent a novel mode of action as a cytokine.

In the present study, we demonstrate that the urinary excretion of GGT changes in parallel with established biochemical markers of bone resorption, NTX and DPD, and therefore reflects bone resorption activity both in animal models and human subjects. Whereas serum GGT activity derives mainly from the liver, GGT is most abundantly expressed in the proximal tubule of the kidney, where this ectoenzyme is located

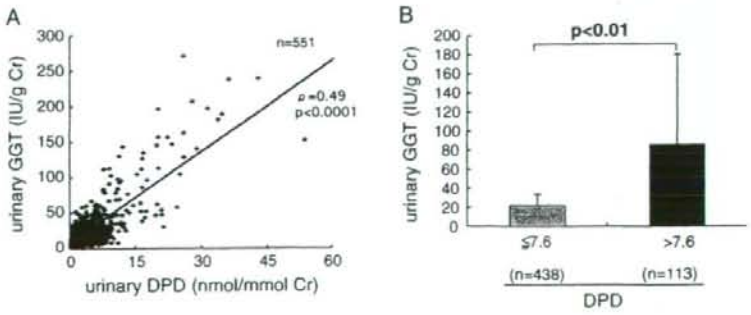

Fig. 5. Correlation between urinary GGT and DPD excretion in postmenopausal women. (A) In 551 postmenopausal women (50–89 years old; mean age, 66), urinary excretion of GGT showed a highly positive correlation with urinary DPD ($p<0.0001$). (B) Of these individuals, 113 showed elevated bone resorption (DPD >7.6 nmol/mmol Cr); and their urinary GGT excretion was increased significantly compared with that of the individuals with lower DPD values ($p<0.01$).

on the apical membrane [23]. Although the exact mechanism underlying GGT excretion in high bone turnover states remains to be determined, increased GGT activity in the urine of humans as well as experimental animals with accelerated bone resorption, without appreciable increase in serum concentrations, prompts us to hypothesize that the GGT anchored to the plasma membrane of renal tubular cells and exposed to the tubular lumen is prone to being shed into the urine in response to some signaling cue from bone turnover. Communication between bone and kidney is known for collagen cross-links; the conversion of peptide bound to free DPD in the kidney has been reported to become more efficient as bone turnover decreases [15].

By fractionation we found that most of the GGT activity in human urine was recovered in the pellet fraction after centrifugation at 200,000×*g*, suggesting that GGT is not excreted in a soluble form but rather in association with certain microstructures. A recent proteomic analysis of exosomes [membrane vesicles that originate as internal vesicles of multivesicular bodies (MVBs)] in the urine identified protein components of MVBs, among which GGT was included [19]. Taken together with our observations, it is tempting to speculate that increased GGT activity in a high bone turnover state is associated with exosomes and the shedding of exosomal GGT from the proximal renal tubules is stimulated in response to some cue from elevated bone resorption [25]. This may provide an explanation for the unexpected observation that unlike serum GGT activity, which is stable after freezing at −20°C and thawing, most of the urinary GGT activity is lost after freezing at −20°C. Alternatively, the possibility that GGT is produced in bone sites undergoing elevated resorption and is excreted in the urine after filtration through the glomerulus cannot be completely ruled out, although it seems unlikely that GGT, with a relatively high molecular weight, is filtered through the glomerulus under physiological conditions. Further studies are required to identify the molecular form(s) of GGT in the urine, and to clarify the specific mechanism(s) by which its excretion is enhanced in diseases with elevated osteoclastic activity.

Osteoporosis is pandemic in industrialized countries, and early diagnosis with timely measures is crucial for mitigating further bone loss and preventing bone fracture [1,13]. The widely used measurement of BMD alone is not sufficient for assessing fracture risk and can miss most of the postmenopausal women who experience fracture [22]. In addition to BMD, several other factors are known to impact the quality of bone, including bone geometry and microstructure, microdamage, and bone turnover, but only biochemical markers of bone turnover are available for use in clinical practice [5]. Measurement of these biochemical markers, however, is time consuming and costly, and a simple and inexpensive method for mass screening is urgently required. Since GGT activity can be measured inexpensively in-house for large numbers of patients in a very short time with little variability, the measurement of the GGT urinary level may provide a highly convenient and useful method for screening individuals who have increased bone turnover and therefore an increased risk for bone fracture. It is to be noted that since urinary GGT activity can be increased in renal dysfunction due to drug intoxication, diabetes and hypertensive nephropathy [3,26,27], the results should be interpreted with caution.

Acknowledgments

We thank Dr. Sunao Takeshita (NCGG) for the valuable suggestions on the manuscript and the figures, Mr. Atsushi Nomura (Enkaku Medical Co. Ltd., Nagoya, Japan) for measuring DPD levels, Dr. Junko Tanaka (Hiroshima University) for help in statistical analysis, and Ms Kumi Tsutsumi (NCGG) for the figure preparation. Pacific Edit reviewed the manuscript prior to submission. This study was supported in part by grants from the programs Comprehensive Research on Aging and Health (to K.I.) and Research on Dementia and Fracture (to S.N.) from the Ministry of Health, Labor, and Welfare of Japan and from the Program for Promotion of Fundamental Studies in Health Sciences of the National Institute of Biomedical Innovation (NIBIO) of Japan (MF-14 to K.I.).

References

[1] Osteoporosis prevention, diagnosis, and therapy. JAMA 2001;285:785–95.
[2] Boyle WJ, Simonet WS, Lacey DL. Osteoclast differentiation and activation. Nature 2003;423:337–42.
[3] Cheung CK, Yeung VT, Cockram CS, Swaminathan R. Urinary excretion of albumin and enzymes in non-insulin-dependent Chinese diabetics. Clin Nephrol 1990;34:125–30.
[4] Delmas PD. Treatment of postmenopausal osteoporosis. Lancet 2002;359:2018–26.
[5] Delmas PD, Eastell R, Garnero P, Seibel MJ, Stepan J. The use of biochemical markers of bone turnover in osteoporosis. Committee of Scientific Advisors of the International Osteoporosis Foundation. Osteoporos Int 2000;11(Suppl 6):S2–S17.
[6] Garnero P, Hausherr E, Chapuy MC, Marcelli C, Grandjean H, Muller C, et al. Markers of bone resorption predict hip fracture in elderly women: the EPIDOS Prospective Study. J Bone Miner Res 1996;11:1531–8.
[7] Hanson DA, Weis MA, Bollen AM, Maslan SL, Singer FR, Eyre DR. A specific immunoassay for monitoring human bone resorption: quantitation of type I collagen cross-linked N-telopeptides in urine. J Bone Miner Res 1992;7:1251–8.
[8] Ito M, Ikeda K, Nishiguchi M, Shindo H, Uetani M, Hosoi T, et al. Multi-detector row CT imaging of vertebral microstructure for evaluation of fracture risk. J Bone Miner Res 2005;20:1828–36.
[9] Kanis JA. Diagnosis of osteoporosis and assessment of fracture risk. Lancet 2002;359:1929–36.
[10] Levasseur R, Barrios R, Elefteriou F, Glass II DA, Lieberman MW, Karsenty G. Reversible skeletal abnormalities in gamma-glutamyl transpeptidase-deficient mice. Endocrinology 2003;144:2761–4.
[11] Lieberman MW, Barrios R, Carter BZ, Habib GM, Lebovitz RM, Rajagopalan S, et al. gamma-Glutamyl transpeptidase. What does the organization and expression of a multipromoter gene tell us about its functions? Am J Pathol 1995;147:1175–85.
[12] Lieberman MW, Wiseman AL, Shi ZZ, Carter BZ, Barrios R, Ou CN, et al. Growth retardation and cysteine deficiency in gamma-glutamyl transpeptidase-deficient mice. Proc Natl Acad Sci U S A 1996;93:7923–6.
[13] Mazanec D. Osteoporosis screening: time to take responsibility. Arch Intern Med 2004;164:1047–8.
[14] McClung MR, Lewiecki EM, Cohen SB, Bolognese MA, Woodson GC, Moffett AH, et al. Denosumab in postmenopausal women with low bone mineral density. N Engl J Med 2006;354:821–31.
[15] Naylor KE, Jackson B, Eastell R. The renal clearance of free and peptide-bound deoxypyridinoline: response to pamidronate treatment of Paget's disease. J Bone Miner Res 2003;18:658–61.
[16] Niida S, Kawahara M, Ishizuka Y, Ikeda Y, Kondo T, Hibi T, et al. Gamma-

glutamyltranspeptidase stimulates receptor activator of nuclear factor-kappaB ligand expression independent of its enzymatic activity and serves as a pathological bone-resorbing factor. J Biol Chem 2004;279:5752–6.
[17] Niida S, Kondo T, Hiratsuka S, Hayashi S, Amizuka N, Noda T, et al. VEGF receptor 1 signaling is essential for osteoclast development and bone marrow formation in colony-stimulating factor 1-deficient mice. Proc Natl Acad Sci U S A 2005;102:14016–21.
[18] Orimo H, Hayashi Y, Fukunaga M, Sone T, Fujiwara S, Shiraki M, et al. Diagnostic criteria for primary osteoporosis: year 2000 revision. J Bone Miner Metab 2001;19:331–7.
[19] Pisitkun T, Shen RF, Knepper MA. Identification and proteomic profiling of exosomes in human urine. Proc Natl Acad Sci U S A 2004;101:13368–73.
[20] Robins SP, Woitge H, Hesley R, Ju J, Seyedin S, Seibel MJ. Direct, enzyme-linked immunoassay for urinary deoxypyridinoline as a specific marker for measuring bone resorption. J Bone Miner Res 1994;9:1643–9.
[21] Seeman E. Pathogenesis of bone fragility in women and men. Lancet 2002;359:1841–50.
[22] Siris ES, Chen YT, Abbott TA, Barrett-Connor E, Miller PD, Wehren LE, et al. Bone mineral density thresholds for pharmacological intervention to prevent fractures. Arch Intern Med 2004;164: 1108–1112.
[23] Taniguchi N, Ikeda Y. gamma-Glutamyl transpeptidase: catalytic mechanism and gene expression. Adv Enzymol Relat Areas Mol Biol 1998;72:239–78.
[24] Teitelbaum SL. Bone resorption by osteoclasts. Science 2000;289:1504–8.
[25] Thery C, Zitvogel L, Amigorena S. Exosomes: composition, biogenesis and function. Nat Rev, Immunol 2002;2:569–79.
[26] Zafirovska KG, Bogdanovska SV, Marina N, Gruev T, Lozance L. Urinary excretion of three specific renal tubular enzymes in patients treated with nonsteroidal anti-inflammatory drugs (NSAID). Ren Fail 1993;15:51–4.
[27] Zuppi C, Baroni S, Scribano D, Di Salvo S, Musumeci V. Choice of time for urine collection for detecting early kidney abnormalities in hypertensives. Ann Clin Biochem 1995;32(Pt 4):373–8.

J Neurosurg Spine 4:509–513, 2006

Recurrence of hypertrophic spinal pachymeningitis

Report of two cases and review of the literature

ZENYA ITO, M.D., YOSHIMITSU OSAWA, M.D., YUKIHIRO MATSUYAMA, M.D., TAKAAKI AOKI, M.D., ATSUSHI HARADA, M.D., AND NAOKI ISHIGURO, M.D.

Department of Orthopedic Surgery, Nagoya First Red Cross Hospital; Department of Orthopedic Surgery, Nagoya University School of Medicine, Nagoya; and Department of Orthopedic Surgery, National Center for Geriatrics and Gerontology, Obu, Aichi, Japan

✓ Hypertrophic spinal pachymeningitis (HSP) is a comparatively rare disease characterized by hypertrophic inflammation of the dura mater and clinical symptoms that progress from local pain to myelopathy. The authors report two cases of recurrent HSP and review the English- and Japanese-language literature focusing on the recurrence of HSP.

In the first case, a man who presented at 67 years of age with lower-extremity numbness, gait disturbance, and bladder dysfunction experienced two recurrences of HSP during the 11 years of follow up after his initial laminectomy. Both recurrences were successfully treated with laminoplasty and duraplasty. Three years after his last surgical procedure, he was still able to walk with the aid of a walker. In the second case, a man who presented at 62 years of age with lower-extremity numbness and gait disturbance was initially treated successfully with steroid pulse therapy. Approximately 8 months after his initial presentation, his symptoms recurred. He underwent laminoplasty and duraplasty. At the 2.5-year follow-up examination, he had only mild neurological deficits and was still able to walk unaided.

To explore possible causes of recurrence, the authors searched the English- and Japanese-language literature for cases of HSP. Of the 96 cases identified, 11 were recurrent. Data on the presence or absence of inflammatory signs were available for 84 patients. A chi-square analysis revealed a significantly increased rate of recurrence for patients who had at least one positive inflammatory sign before surgery (six [20%] recurrent cases of 30) compared with those who had no positive inflammatory signs before surgery (two [3.7%] recurrent cases of 54) ($p < 0.05$). The authors conclude that HSP recurrence occurs because of active inflammation of the dura before surgery and the influence of chronic inflammation, including residual arachnoiditis.

KEY WORDS • **dura mater** • **disease recurrence** • **hypertrophy** • **arachnoiditis** • **hypertrophic spinal pachymeningitis** • **spinal lesion**

HYPERTROPHIC spinal pachymeningitis is a comparatively rare disease characterized by hypertrophic inflammation of the dura mater and a clinical course that progresses from local pain to myelopathy.[2,4] The cause and natural history of HSP are not well understood. Since it was first reported by Charcot and Joffroy[3] in 1869, few articles related to this disease have been published in the medical literature. Furthermore, the authors of most of these articles limited their focus to a short period after initial treatment and did not include information on recurrence. In the present article we report two cases of recurrent HSP. In addition, we review the English- and Japanese-language literature focusing on the recurrence of HSP.

Abbreviations used in this paper: HSP = hypertrophic spinal pachymeningitis; MR = magnetic resonance.

Case Reports

Case 1

First Examination, Operation, and Outcome. This man with chronic back pain was admitted to our hospital in October 1993 at age 67 years, complaining of lower-extremity numbness, gait disturbance, and bladder dysfunction. The muscle power in his right and left lower extremities were Grades 3/5 and 2/5, respectively. A sensory disturbance of pain and touch was found below T-8. The patient had no fever, and his erythrocyte sedimentation rate was 53 mm/hour. The results of serological tests, including white blood cell count and C-reactive protein level measurement, were within normal ranges. Cerebrospinal fluid values were also within the normal range. Magnetic resonance imaging showed that the spinal cord had been compressed between T-6 and T-7 in the dorsal and ventral portions (Fig. 1). Although epidural abscess or

tumor was suspected, we were unable to establish a definite diagnosis before surgery. A laminectomy was performed at the T6–8 level in December 1993. The dura mater was found to be thickened (~ 3 mm), with marked adhesion of epidural fat. After the dura mater constricting the spinal cord was removed, duraplasty was performed. Microscopic examination of sections of the excised dura revealed the presence of plasma cells and infiltrated lymphocytes (Fig. 2). We considered the findings to be compatible with a diagnosis of HSP. Two months postoperatively, the patient could walk unaided.

Second Examination, Operation, and Outcome. In August 1997, the patient's back pain and bladder dysfunction recurred, and on December 30, numbness of the lower extremities and gait disturbance developed. Two weeks later, MR imaging revealed thickened dura mater compressing the spinal cord at the T3–4 level. On January 29, 1998, laminoplasty and duraplasty were performed. Histological examination of dural sections revealed the same pathological findings as had been previously observed. Within two months of surgery, the patient was able to walk with a cane.

Third Examination, Operation, and Outcome. In February 2000, the patient presented with numbness of the upper extremities, and complained of weakness and numbness of fingers in both hands as well as gait disturbance. Three weeks later, MR imaging revealed thickened dura mater at C-6 to T-1. On May 9, laminoplasty and duraplasty were performed, and the same histopathological findings were noted. Postoperative cervical MR imaging showed cord decompression. Three years later, the patient was still able to walk with the aid of a walker.

Case 2

First Examination and Treatment. This man presented with lower-extremity numbness and gait disturbance in September 2000 at age 62 years. The muscle power in his lower extremities was almost normal, but he had reduced sensation of pain and touch below the T-6 level. Like the patient in Case 1, this patient had no fever, and results of his serological and cerebrospinal fluid tests were within the normal range. Spinal MR imaging revealed hypertrophic dura mater and cord compression at the T1–5 level (Fig. 3). Steroid pulse therapy (9300 mg) was administered. Three weeks later the patient's condition had improved, and another set of MR images showed that the thickened dura had become thinner. By November, the patient was able to walk with a cane.

Second Examination, First Operation, and Outcome. The following May, the patient was admitted to the hospital, again complaining of gait disturbance. Examination revealed that sensation was diminished at the T-6 level. We considered that he might be suffering from recurrence of HSP in the area in which it had been observed in the pretreatment MR images, and on June 12 performed a C6–T5 laminoplasty and duraplasty. We found the dura mater to be approximately 7 mm thick. Histological examination of sections of the thickened dura revealed nonspecific chronic inflammation. At follow up 2.5 years after surgery, the patient had only mild neurological deficit and could walk unaided.

Discussion

Hypertrophic spinal pachymeningitis is a comparatively rare disease. According to Charcot and Joffroy,[3] its clinical progression may be viewed in three stages: in the first stage, patients experience local and radicular pain; in the second stage, signs of nerve root compression are present; and in the third stage, patients suffer from signs and symptoms of spinal cord compression. Elsberg[7] has indicated that HSP should be suspected when a patient with spinal cord compression has radicular pain in three or more nerve root regions. There have been many case reports in which the authors have documented short-term results.[2,5,6]

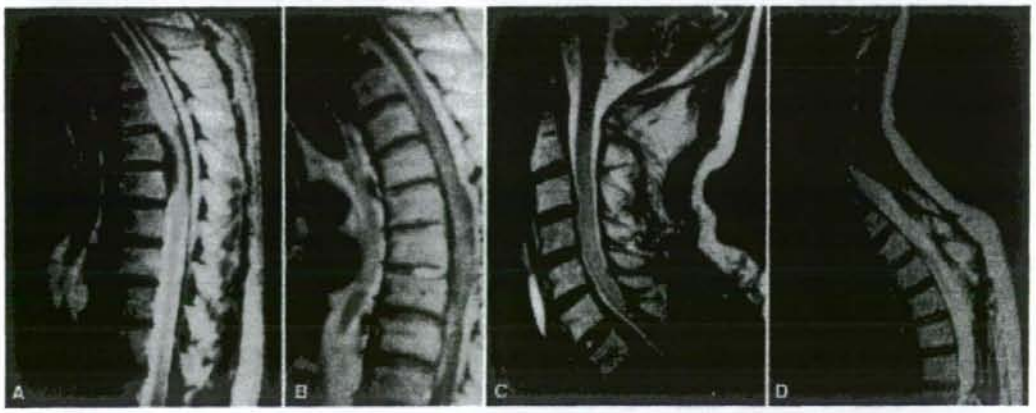

FIG. 1. Case 1. Preoperative and postoperative MR images. A: Sagittal T_2-weighted sequence obtained before the first operation, revealing dorsal and ventral T6–7 cord compression. B: Sagittal Gd-enhanced sequence obtained before the second operation, revealing HSP at the T3–5 level. C: Sagittal T_2-weighted sequence obtained before the third operation, revealing thickened dura at C-6 to T-1. D: Sagittal T_2-weighted sequence obtained after the third operation, revealing decompression of the entire lesion area.

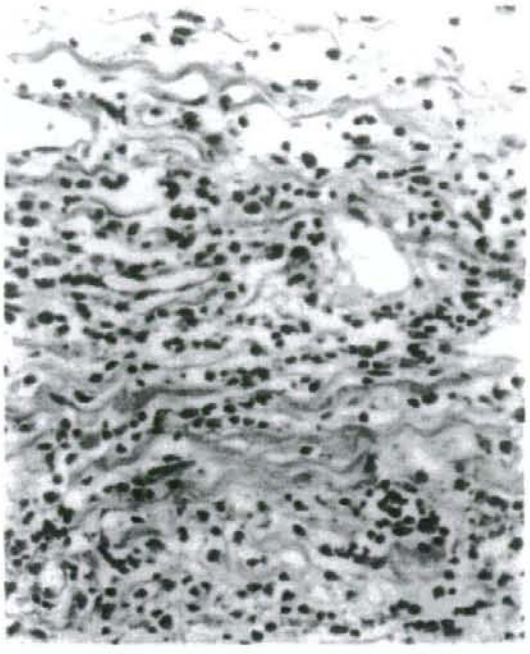

FIG. 2. Photomicrograph of a section of the excised dura mater, showing plasma cells and infiltrating lymphocytes. Whether the arachnoid mater was infiltrated is unclear. H & E, original magnification × 400.

[14,19,22–25] Mikawa and coauthors[17] identified 52 cases in their review of the English- and Japanese-language literature; however, none of the published studies focused on the recurrence of HSP or its possible causes, and few authors reported the long-term course of the disease. To our knowledge, the present article is the first to address specifically the recurrence of HSP.

Park and associates[21] reported that the presence of a residual mass after surgery to treat a ventral lesion of the dura mater. Juhasz[12] found that the inflammatory process did not have definite limits in the caudal and cranial directions and that the inflammation frequently extended to the internal surface of the dura. Based on these observations, it has been proposed that residual inflammation from the irremovable ventral part of the dural lesion leads to recurrence. To test this hypothesis, we searched the PubMed and Cochrane Library databases for reports of cases of HSP by using "hypertrophica," "pachymeningitis," and "recurrence" as search terms. We identified 96 cases (46 of which were described in English and 50 in Japanese), including the two in the present study. Eleven (11%) of the 96 cases involved recurrence (six cases with one recurrence and five with two; Table 1).[1,9,12,13,15–18]

We initially divided the HSP cases into two groups based on recurrence, a nonrecurrence group (85 cases) and a recurrence group (11 cases), and compared them. In the recurrence group, the mean period from the first conservative therapy or surgery to the first recurrence was 1.3 years (range 1 week–4 years). In five of these cases, the lesion recurred twice, and the average time between the first and second recurrence in this subset was 11.3 months (range 3 months–2 years). A two-tailed t-test revealed no significant intergroup difference, except for the duration of the mean follow-up period (Table 2).

We then performed three subgroup analyses. For the first subgroup analysis, we divided the cases into two groups based on the presence or absence of inflammatory signs: 1) a noninflammatory group, which comprised those patients in whom inflammatory signs, including fever, increased erythrocyte sedimentation rate, leukocytosis, and increased C-reactive protein level, were absent before surgery; and 2) an inflammatory group, which comprised those patients who had at least one inflammatory sign. Cases in which there was no mention of inflammation were excluded from this second analysis. The noninflammatory group included a total of 54 cases of HSP, of which two were recurrent. The inflammatory group included a total of 30 cases, of which six were recurrent. A chi-square analysis revealed a statistically significant intergroup difference ($p < 0.05$; Fig. 4).

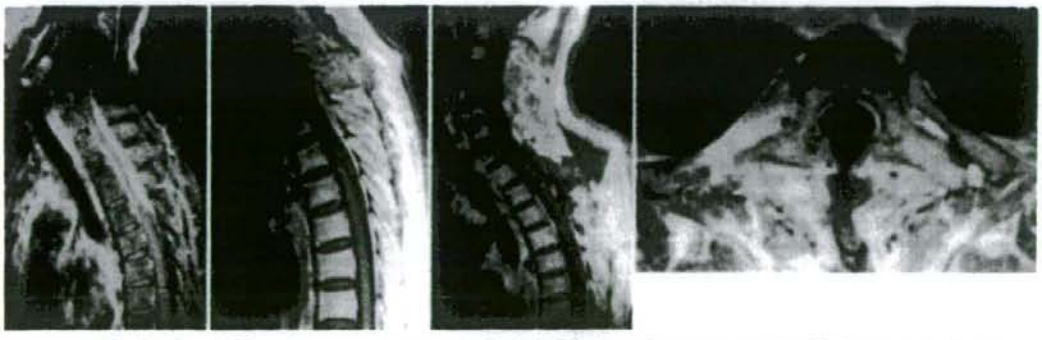

FIG. 3. Case 2. Magnetic resonance images. A: Sagittal Gd-enhanced sequence, revealing HSP at the T1–5 level in the dorsal and ventral dura mater. B: Sagittal Gd-enhanced sequence, showing the same HSP lesion after steroid therapy. C: Sagittal Gd-enhanced sequence obtained after surgery, showing that virtually all of the thickened dura had been removed. D: Axial Gd-enhanced sequence obtained after surgery, demonstrating no dural thickening.

TABLE 1

*Characteristics of 11 patients with recurrent HSP**

Authors & Year	Age (yrs), Sex	Involved Level	Ventral Lesion	Op†	Duration‡	Outcome	FU (yrs)
Juhasz, 1950	16, F	T7–8	—	laminectomy			
1st recurrence		T7–8	—	laminectomy	6 mos	recovered	2.4
Guidetti & La Torre, 1967	15, M	T6–9	—	durotomy			
1st recurrence		C4–T3	—	durotomy	3 yrs	recovered	14
Guidetti & La Torre, 1967	65, F	T4–6	—	durotomy			
1st recurrence		T4–6	—	NST	4 yrs	—	4
Adler, et al., 1991	47, M	T8–11	—	laminectomy			
1st recurrence		C2–7	yes	laminectomy	4 yrs		
2nd recurrence		T1–7	—	laminectomy	2.5 mos	recovered	7
Mikawa, et al., 1994	58, F	T1–11	yes	laminectomy			
1st recurrence		C-7	yes	durotomy	2 wks		
2nd recurrence		C3–6	yes	durotomy	3 mos	recovered	0.5
Kanamori, et al., 1997	28, M	T5–L2	yes	laminectomy			
1st recurrence		T2–?	—	NST	4 mos	recovered	4.2
Mihara, et al., 1997	54, F	T10–12	yes	dura incision			
1st recurrence		T-9	yes	dura incision	1 wk		
2nd recurrence		T-9	yes	durotomy	3 mos	unchanged	0.6
Nagashima, 2001	53, F	C7–T1	yes	laminectomy			
1st recurrence		C7–T7	yes	dura incision	2 mos		
2nd recurrence		T1–8	yes	NST	1 yr, 10 mos	died	2.6
Khadilkar, et al., 2003	42, F	C1–4	yes	durotomy			
1st recurrence		C2–4	yes	NST	1 yr, 3 mos	recovered	5
present study							
Case1	67, M	T6–8	yes	durotomy			
1st recurrence		T3–5	yes	durotomy	3 yrs, 6 mos		
2nd recurrence		C4–T2	yes	durotomy	2 yrs	recovered	10
Case 2	62, M	T1–5	yes	ST			
1st recurrence		C6–T5	yes	durotomy	5 mos	recovered	3

* FU = follow up; NST = nonsurgical treatment; ST = steroid therapy; — = not known.

† Surgery was performed using various methods: laminectomy only, dura incision only, and durotomy with artificial dura mater or fascia.

‡ Duration indicates the time from therapy to recurrence.

For the next subgroup analysis, we compared the cases in which patients underwent durotomy or duraplasty and those in which patients underwent laminectomy alone or only incision, not removal, of the dura mater. The former group included 37 cases of HSP, eight of which were recurrent. The latter group consisted of 41 cases, eight of which were recurrent. The difference was not statistically significant.

For our final subgroup analysis, we divided the cases into those in which both ventral and dorsal inflammation or hypertrophy of the dura mater was documented on pathological, myelography, or MR imaging examination, and those in which only dorsal inflammation or hypertrophy was documented. The former group included 25 cases, eight of which were recurrent. The latter group included five cases, none of which was recurrent. The difference was not statistically significant.

From these results, we concluded that recurrence was not caused by a residual lesion but by active inflammation of the dura mater that was already present before surgery. We considered the possible role of arachnoiditis as an additional cause of recurrence. Friedman and Flanders[8] reported that the peripheral margin in a case of pachymeningitis was enhanced on MR imaging and was unusually close to the highly vascularized arachnoid mater. Oohishi and associates[20] found that this disease process was not just confined to the dura, but also involved the arachnoid mater and pia mater (trimeningitis). Juhasz[12] suggested that HSP associated with arachnoiditis is separate from the arachnoid mater, because the lateral aspect of the dura was found to be relatively intact. Considering that inflammation is often found in the arachnoid as well as the dura, residual arachnoiditis above or below the resected area of the dura mater might cause recurrence, even if the visibly hypertrophic part of the dura is removed. Patients were treated with steroid therapy in 13 cases, some

TABLE 2

*Characteristics and outcome data for 96 cases of HSP with and without recurrence**

Variable	Recurrence	No recurrence
no. of cases	11	85
mean age (yrs)†	46.1 ± 18.8	48.7 ± 15.9
sex (no. of patients)		
Male	5	48
Female	6	37
mean no. of levels involved (range)	3.9 (2–10)	4.2 (1–24)
mean dura thickness (mm) (range)	4.8 (2–8)	6.6 (1–20)
outcome (no. of patients)		
recovered	9	55
unchanged	1	11
died	1	16
unknown	0	3
FU period	4.8 ± 4.1	1.4 ± 2.6

* The difference between groups was significant only for the duration of the average follow-up period ($p < 0.0005$).

† Values are given as means ± standard deviation.

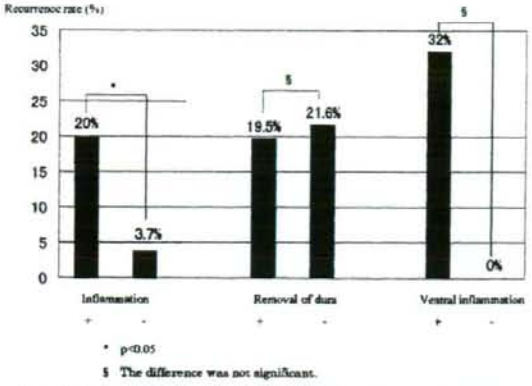

FIG. 4. Bar graph depicting the results of analyses of HSP recurrence rates. Cases with sufficient data were included in the following subgroup comparative analyses: 1) presence or lack of at least one positive inflammatory sign; 2) removal or retention of dura; and 3) presence or lack of ventral inflammation of the dura mater. See *Discussion* for the numbers of patients in each group.

of which, including ours, were recurrent,[1,6,11,13,15,17,18,22] but many of the authors who reported treating patients with steroid agents claimed that the effect was not certain. Hatano and coworkers[10] found that patients with a linear pattern of dural enhancement responded better to corticosteroid therapy than those with a nodular pattern of enhancement. As a result of our analyses of the available data, we conclude that surgical decompression by laminectomy or durotomy and duraplasty is to be recommended for this disease.

Guidetti and La Torre[9] have suggested that removal of the posterior surface of the dura mater beyond the apparent limits of the lesion might be useful in controlling recurrence. In conclusion, we consider that recurrence occurs due to active dural inflammation present before surgery and the influence of chronic inflammation, including residual arachnoiditis.

References

1. Adler JR, Sheridan W, Kosek J, Linder S: Pachymeningitis associated with a pulmonary nodule. **Neurosurgery 29:** 283–287, 1991
2. Ashkenazi E, Constantini S, Pappo O, Gomori M, Averbuch-Heller L, Umansky F: Hypertrophic spinal pachymeningitis: report of two cases and review of the literature. **Neurosurgery 28:**730–732, 1991
3. Charcot JM, Joffroy A: Deux cas d'atrophie musculaire progressive avec lesions de la substance grise et des faisceaux anterolateraux de la moelle epiniere. **Arch Physiol Norm Path 2:** 354–367; 744–760, 1869
4. Deshpande DH, Vidyasagar D: Hypertrophic pachymeningitis dorsalis. **Surg Neurol 12:**217–220, 1979
5. Digman KE, Partington CR, Graves VB: MR imaging of spinal pachymeningitis. **J Comput Assist Tomogr 14:**988–990, 1990
6. Dumont AS, Clark AW, Sevick RJ, Myles ST: Idiopathic hypertrophic pachymeningitis: a report of two patients and review of literature. **Can J Neurol Sci 27:**333–340, 2000
7. Elsberg CA: **Tumor of the Spinal Cord.** New York: PB Hoeber, 1925, pp 342–343
8. Friedman DP, Flanders AE: Enhanced MR imaging of hypertrophic pachymeningitis. **AJR Am J Roentgenol 169:** 1425–1428, 1997
9. Guidetti B, La Torre E: Hypertrophic spinal pachymeningitis. **J Neurosurg 26:**496–503, 1967
10. Hatano N, Behari S, Nagatani T, Kimura M, Ooka K, Saito K, et al: Idiopathic hypertrophic cranial pachymeningitis: clinicoradiological spectrum and therapeutic options. **Neurosurgery 45:**1336–1344, 1999
11. Ideguchi H, Hosoda H, Gondo G, Ono A: [Spinal pachymeningitis.] **Sekitsuisekizui 14:**420–422, 2001 (Jpn)
12. Juhasz P: Contributions to the clinical aspects and to the pathoanatomy of pachymeningitis spinalis externa. **Monatsschr Psychiatr Neurol 120:**152–168, 1950
13. Kanamori M, Matsui H, Terahata N, Tsuji H: Hypertrophic spinal pachymeningitis. A case report. **Spine 22:**1787–1790, 1997
14. Kao KP, Huang CI, Shan DE, Ho JT, Chang T, Chu FL: Non-obstructive idiopathic pachymeningitis cervicalis hypertrophica. **J Neurol Neurosurg Psychiatry 49:**1441–1444, 1986
15. Khadilkar SV, Menezes K, Parekh HN, Urskar M, Bhagwati SN: Idiopathic hypertrophic cervical pachymeningitis: case report with 5 year follow-up. **J Assoc Physicians India 51:** 391–393, 2003
16. Mihara H, Hachiya M, Oonari K, Hujii H, Okubo T, Yamada K: [Complete paraplegia due to hypertrophic pachymeningitis of thoracic spine.] **Kanagawa Seisaishi 10:**165–169, 1997 (Jpn)
17. Mikawa Y, Watanabe R, Hino Y, Hirano K: Hypertrophic spinal pachymeningitis. **Spine 19:**620–625, 1994
18. Nagashima T: [Neuropathology of hypertrophic pachymeningitis.] **Shinkeinaika 55:**207–215, 2001 (Jpn)
19. Nishida K, Baba I, Sumida T, Ishida T, Murakami T , Ohishi Y, et al: [Hypertrophic pachymeningitis of the cervical spine. A case report.] **Tyuyonseikaishi 10:**213–216, 1998 (Jpn)
20. Oohishi T, Ishiko T, Arai M, Kase M, Matsushita M: Pachymeningitis cervicalis hypertrophica. **Acta Pathol Jpn 32:** 163–171, 1982
21. Park SH, Whang J, Sohn M, Chui Oh Y, Lee CH, Whang YJ: Idiopathic hypertrophic spinal pachymeningitis: a case report. **J Korean Med Sci 16:**683–688, 2001
22. Rosenfeld JV, Kaye AH, Davis S, Gonzales M: Pachymeningitis cervicalis hypertrophica. Case report. **J Neurosurg 66:** 137–139, 1987
23. Sato E, Kohno H, Nakashima I: [Hypertrophic spinal pachymeningitis in the thoracolumbar region: a case report.] **Kantouseisaishi 29:**116–120, 1998 (Jpn)
24. Sharma V, Newton G, Wahal KM: Idiopathic hypertrophic pachymeningitis—an uncommon cause of cord compression. **Indian J Pathol Microbiol 35:**133–136, 1992
25. Wirth FP Jr, Gado M: Incomplete myelographic block with hypertrophic spinal pachymeningitis. Case report. **J Neurosurg 38:**368–370, 1973

Manuscript received June 3, 2005.
Accepted in final form March 24, 2006.

Address reprint requests to: Zenya Ito, M.D., Department of Orthopedic Surgery, Nagoya First Red Cross Hospital, 47-1-102 Takikawa-cho, Showa-ku, Nagoya, Aichi, Japan. email: z.ito@nifty.ne.jp.

Minodronate Suppresses Prostaglandin F2α-induced Vascular Endothelial Growth Factor Synthesis in Osteoblasts

Y. Hanai[1,2]
H. Tokuda[1,2]
S. Takai[1]
A. Harada[3]
T. Ohta[4]
O. Kozawa[1]

Abstract

In our previous study, we showed that prostaglandin $F_{2\alpha}$ ($PGF_{2\alpha}$) stimulates vascular endothelial growth factor (VEGF) synthesis via activation of p44/p42 mitogen-activated protein (MAP) kinase via protein kinase C (PKC) in osteoblast-like MC3T3-E1 cells. In addition, we demonstrated that incadronate amplified, and tiludronate suppressed $PGF_{2\alpha}$-induced VEGF synthesis among bisphosphonates, while alendronate or etidronate had no effect. In the present study, we investigated the effects of minodronate, a newly developed bisphosphonate, on $PGF_{2\alpha}$-induced VEGF synthesis in MC3T3-E1 cells. Minodronate significantly reduced VEGF synthesis induced by $PGF_{2\alpha}$ dose-dependently at levels between 3 and 100 μM. $PGF_{2\alpha}$-stimulated phosphorylation of Raf-1, MEK1/2 and p44/p42 MAP kinase were suppressed by minodronate. 12-*O*-tetradecanoylphorbol-13-acetate (TPA), a direct activator VEGF synthesis induced by PKC, was inhibited by minodronate. Minodronate inhibited Raf-1, MEK1/2 and p44/p42 MAP kinase phosphorylation induced by TPA. Mevalonate failed to affect the suppressive effect of minodronate on $PGF_{2\alpha}$-induced VEGF synthesis. Taken together, these results indicate that minodronate suppresses $PGF_{2\alpha}$-stimulated VEGF synthesis at the point between PKC and Raf-1 in osteoblasts.

Key Words
Bisphosphonate · prostaglandin $F_{2\alpha}$ · vascular endothelial growth factor · osteoblast

Introduction

Osteoblasts and osteoclasts are main functional cells that regulate bone metabolism. The former is responsible for bone formation, and the latter for bone resorption [1]. Bone-remodeling results from this finely coordinated process of bone resorption by activated osteoclasts coupled with subsequent deposition of new matrix by osteoblasts. Several bone-resorptive agents such as parathyroid hormone and 1,25-$(OH)_2$ vitamin D_3 upregulate RANKL (receptor activator of nuclear factor κB ligand) expression by binding specific receptors on osteoblasts, suggesting that osteoblasts also play crucial roles in the regulation of bone resorption [2]. During these processes, capillary endothelial cells along with microvasculature with osteoblasts and osteoprogenitor cells, which locally proliferate and differentiate into osteoblasts, migrate into the resorption lacuna. Therefore, osteoblasts, osteoclasts and capillary endothelial cells cooperatively regulate bone metabolism in a closely coordinated fashion via humoral factors as well as by direct cell-to-cell contact [3].

Affiliation
[1] Department of Pharmacology, Gifu University Graduate School of Medicine, Gifu, Japan
[2] Department of Clinical Laboratory, National Hospital for Geriatric Medicine, National Center for Geriatrics and Gerontology, Aichi, Japan
[3] Functional Restoration, National Hospital for Geriatric Medicine, National Center for Geriatrics and Gerontology, Aichi, Japan
[4] Internal Medicine, National Hospital for Geriatric Medicine, National Center for Geriatrics and Gerontology, Aichi, Japan

Correspondence
Osamu Kozawa · Department of Pharmacology · Gifu University Graduate School of Medicine · 1-1 Yanagido · Gifu 501-1194 · Japan · Phone: +81 (58) 230-6214 · Fax: +81 (58) 230-6215 · E-Mail: okozawa@cc.gifu-u.ac.jp

Received 12 July 2005 · **Accepted after revision** 7 December 2005

Bibliography
Horm Metab Res 2006; 38: 152–158 © Georg Thieme Verlag KG Stuttgart · New York ·
DOI 10.1055/s-2006-925177 · ISSN 0018-5043

Bisphosphonate, a stable analogue of pyrophosphate, is generally known as an inhibitor of bone resorption [4]. Bisphosphonates are widely used as a potent agent for the treatment of various metabolic bone diseases associated with increased osteoclastic bone resorption such as Paget's disease, tumoral bone disease, and osteoporosis [4]. Osteoclast recruitment, osteoclastic adhesion to bone surface and osteoclast activity inhibition is known to be the main mechanisms by which bisphosphonates inhibit bone resorptive actions [4]. In addition to osteoclasts, the inhibitory action of bisphosphonates on osteoclasts is reportedly partly mediated through its actions on osteoblasts [5,6]. In osteoblastic cell line CRP 10/30, both ibandronate and alendronate induce the synthesis of an osteoclastic bone resorption inhibitor [7]. In a previous study [8], we reported that tiludronate inhibits interleukin (IL)-6 synthesis in osteoblast-like MC3T3-E1 cells. Etidronate, alendronate, pamidronate and olpadronate prevent apoptosis of murine primary cultured osteoblasts via activation of p44/p42 mitogen-activated protein (MAP) kinase [9]. In cultured human fetal osteoblasts, pamidronate and zoledronate enhance differentiation and bone-forming activities [10]. Pamidronate and zoledronate also reportedly increase mRNA expression for osteoprotegerin in primary human osteoblasts [11]. In UMR-106-01 osteosarcoma cells, pamidronate and clodronate decrease receptor activator of nuclear factor κB ligand (RANKL) [12]. In addition, zoledronate upregulates osteocalcin and bone morphogenetic protein-2 (BMP-2) gene expression in human osteoblast-like cells [13], and decreases membrane RANKL expression by upregulating tumor necrosis factor-α-converting enzyme [14]. These studies led us to speculate that the effects of bisphosphonates on bone metabolism are not only exerted by osteoclasts, but also by osteoblasts. However, the detailed mechanism of bisphosphonate action on osteoblasts has not yet been fully clarified.

Vascular endothelial growth factor (VEGF) is a potent angiogenic factor that induces angiogenesis, endothelial cell proliferation and capillary permeability [15]. Inactivation of VEGF results in the complete suppression of vascular invasion followed by impaired trabecular bone formation and expansion of the hypertrophic chondrocyte zone in the mouse tibial epiphyseal growth plate [16]. Osteoblasts have been reported to produce and secrete VEGF in response to various physiological agonists [15,17]. In our previous studies, we reported that prostaglandin $F_{2\alpha}$ ($PGF_{2\alpha}$), a potent bone resorptive agent, activates both phosphoinositide (PI)-hydrolyzing phospholipase C (PI-phospholipase C) and phosphatidylcholine (PC)-hydrolyzing phospholipase D (PC-phospholipase D) [18,19], recognized as two major physiological protein kinase C (PKC) activation pathways [20,21], in osteoblast-like MC3T3-E1 cells. In addition, we recently showed that $PGF_{2\alpha}$ induces VEGF synthesis and secretion through PKC-dependent activation of p44/p42 MAP kinase in these cells [22]. Furthermore, we have demonstrated that incadronate enhances [22], while tiludronate suppresses [23] $PGF_{2\alpha}$-induced VEGF synthesis through activation [22] or suppression [23] of p44/p42 MAP kinase in osteoblast-like MC3T3-E1 cells, while alendronate or etidronate has little effect [22].

In the present study, we investigated the effect of minodronate, a newly developed nitrogen-containing bisphosphonate, which is structurally different and has a different side chain structure from incadronate, alendronate tiludronate or etidronate, on $PGF_{2\alpha}$-stimulated VEGF synthesis in MC3T3-E1 cells and the mechanism behind it. In contrast to the results from incadronate [22], and identical to those from tiludronate [22], this study will demonstrate that minodronate inhibits $PGF_{2\alpha}$-stimulated VEGF synthesis in these cells, and that the suppressive effect of minodronate is exerted at the point between PKC and Raf-1.

Materials and Methods

Materials

Minodronate was kindly provided by Yamanouchi Pharmaceuticals Co. Ltd. (Tokyo, Japan). $PGF_{2\alpha}$, 12-*O*-tetradecanoylphorbol-13-acetate (TPA) and mevalonate were purchased from Sigma Chemical Co. (St. Louis, MO). Phosphospecific p44/p42 MAP kinase antibodies, p44/p42 MAP kinase antibodies, phosphospecific MEK1/2 antibodies, MEK1/2 antibodies, phosphospecific Raf-1 antibodies and β-actin antibodies were purchased from New England Biolabs, Inc. (Beverly, MA). ECL Western blotting detection system was purchased from Amersham Japan (Tokyo, Japan). Mouse VEGF ELISA kit was purchased from R&D Systems, Inc. (Minneapolis, MN). Other materials and chemicals were obtained from Sigma Chemical Co. (St. Louis, MO) or Nacalai Tesque, Inc. (Kyoto, Japan). $PGF_{2\alpha}$ was dissolved in ethanol. TPA was dissolved in dimethyl sulfoxide. The maximum concentration of ethanol or dimethyl sulfoxide was 0.1%, which did not affect VEGF assay or Western blot analysis.

Cell culture

MC3T3-E1 cells are a clonal osteoblastic cell line derived from newborn mouse calvaria [24], and reportedly form mineralized matrix. In addition, we previously reported that MC3T3-E1 cells secrete osteocalcin [25] and express alkaline phosphatase [26] under our experimental conditions. MC3T3-E1 cells were maintained as previously described [27]. The cells were cultured in α-minimum essential medium (α-MEM) containing 10% fetal calf serum (FCS) at 37°C in a humidified atmosphere of 5% CO_2/95% air. The cells were seeded into 35 mm (5×10^4) or 90 mm (2×10^5) diameter dishes in α-MEM containing 10% FCS. After five days, the medium was exchanged for α-MEM containing 0.3% FCS. The cells were used for experiments after 48 h.

Assay for VEGF

The cells were pretreated with various doses of minodronate or vehicle for 8 h, then stimulated by $PGF_{2\alpha}$ or TPA in 1 ml of α-MEM containing 0.3% FCS for the indicated period. In addition, mevalonate was added 8 h prior to stimulation by $PGF_{2\alpha}$ to investigate the involvement of mevalonate pathway on minodronate inhibition of VEGF synthesis by $PGF_{2\alpha}$. The conditioned medium was collected, and VEGF in the medium was measured by VEGF ELISA kit.

Analysis of p44/p42 MAP kinase, MEK1/2 or Raf-1

The cultured cells were pretreated with various doses of minodronate or vehicle for 8 h, then stimulated by $PGF_{2\alpha}$ or TPA in 4 ml of α-MEM containing 0.3% FCS for the indicated period. The cells were washed twice with phosphate-buffered saline and then lysed, homogenized and sonicated in a lysis buffer containing 62.5 mM Tris/HCl, pH 6.8, 2% sodium dodecyl sulfate

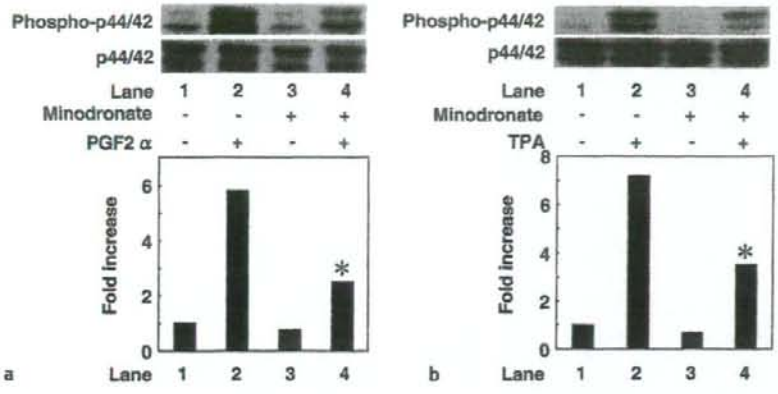

Fig. 1 Effects of minodronate on phosphorylation of p44/p42 MAP kinase induced by PGF2α or TPA in MC3T3-E1 cells. **a** Cultured cells were pretreated with 10 μM minodronate or vehicle for 8 h, then stimulated by 10 μM PGF2α or vehicle for 30 min. **b** The cultured cells were pretreated with 10 μM minodronate or vehicle for 8 h, and then stimulated by 0.1 μM TPA or vehicle for 60 min. Extracts of cells were subjected to SDS-PAGE with subsequent Western blot analysis using antibodies against phospho-specific p44/p42 MAP kinase or p44/p42 MAP kinase. The histogram shows quantitative representations of p44/p42 MAP kinase phosphorylation obtained from laser densitometric analysis. Each value represents the mean of triplicate determinations. Similar results were obtained with two additional and different cell preparations. *$p < 0.05$ compared to the value of PGF2α alone or TPA alone.

(SDS), 50 mM dithiothreitol, and 10% glycerol. SDS-PAGE was performed as described by Laemmli [28] in 10% polyacrylamide gel. Western blotting analysis was performed as described previously [29] using phosphospecific p44/p42 MAP kinase antibodies, p44/p42 MAP kinase antibodies, phosphospecific MEK1/2 antibodies, MEK1/2 antibodies, phosphospecific Raf-1 antibodies or β-actin antibodies, with peroxidase-labeled antibodies raised in goat anti-rabbit IgG used as second antibodies. Peroxidase activity on the nitrocellulose sheet was visualized on x-ray film using the ECL Western blotting detection system.

Determination of absorbance and densitometric analysis

Absorbance of ELISA samples was measured at 450 nm with a microplate spectrophotometer (Bio-Rad Laboratories, Hercules, CA). Densitometric analysis was performed using scanner and image analysis software (image J version 1.32).

Statistical analysis

Data were analyzed by ANOVA followed by Bonferroni's method for multiple comparisons between pairs, and values of $p < 0.05$ were considered significant. All data are presented as the mean ± SD from triplicate determinations. Each experiment was repeated three times with similar results.

Results

Effect of minodronate on PGF2α-induced VEGF synthesis in MC3T3-E1 cells

Recently, we have reported that $PGF_{2\alpha}$ induces VEGF synthesis in osteoblast-like MC3T3-E1 cells, and that incadronate amplifies VEGF synthesis while alendronate fails to affect synthesis [22]. Thus, we investigated the effect of minodronate on $PGF_{2\alpha}$-induced VEGF synthesis in these cells. Minodronate alone had little affect on VEGF levels, but significantly suppressed $PGF_{2\alpha}$-induced VEGF synthesis in MC3T3-E1 cells (49.1 ± 1.2 pg/ml for control; 33.1 ± 2.5pg/ml for 10μM minodronate alone, 1142.7 ± 186.5 pg/ml for 10μM $PGF_{2\alpha}$ alone; and 67.0 ± 5.5* pg/ml for 10 μM $PGF_{2\alpha}$ with 10 μM minodronate pretreatment, as measured during stimulation for 48 h; *$p < 0.05$, compared with the value of $PGF_{2\alpha}$ alone). The inhibitory effect of minodronate was dose-dependent between 3 and 100 μM (data not shown). Minodronate almost completely inhibited the $PGF_{2\alpha}$ effect at a dose of 10 μM. We confirmed that the cell number changed little by treatment [$(8.1 \pm 0.2) \times 10^5$ cells before incubation; $(7.9 \pm 0.4) \times 10^5$ cells after 48 h incubation with 100 μM minodronate; $(8.0 \pm 0.3) \times 10^5$ cells after 48 h incubation with vehicle].

Effects of minodronate on PGF2α-induced or TPA-induced phosphorylation of p44/p42 MAP kinase in MC3T3-E1 cells

In a previous study, we have demonstrated that $PGF_{2\alpha}$-induced VEGF synthesis is activated via p44/p42 MAP kinase in a PKC-dependent manner in MC3T3-E1 cells [22]. Therefore, we then investigated the detailed mechanism of minodronate underlying the inhibition of VEGF synthesis. Minodronate, which alone had little effect on phosphorylation of p44/p42 MAP kinase, markedly suppressed $PGF_{2\alpha}$-induced p44/p42 MAP kinase phosphorylation (Fig. **1a**). According to densitometric analysis, minodronate (10 μM) caused a reduction of approximately 65% in the $PGF_{2\alpha}$ effect (*$p < 0.05$, compared with the value of $PGF_{2\alpha}$ alone).

To elucidate whether or not the effect of minodronate is exerted at a point downstream of PKC, we examined the effect of minodronate on phosphorylation of p44/p42 MAP kinase induced by TPA, a direct activator of PKC [30]. Previously, we found that p44/p42 MAP kinase was markedly phosphorylated by TPA by itself [31]. Minodronate significantly reduced p44/p42 MAP kinase phosphorylation stimulated by TPA (Fig. **1b**). According to densitometric analysis, minodronate (10 μM) caused approximately 60% reduction in TPA effect (*$p < 0.05$, compared with the value of TPA alone).

Effect of minodronate on TPA-induced VEGF synthesis in MC3T3-E1 cells

Previously, we reported that TPA alone stimulated VEGF synthesis in osteoblast-like MC3T3-E1 cells [22]. Therefore, we investigated the effect of minodronate on TPA-induced VEGF synthesis. Minodronate significantly reduced TPA-induced syn-

Table 1 Effect of mevalonate minodronate on the TPA-induced VEGF synthesis in MC3T3-E1 cells

Minodronate	*TPA*	*VEGF (pg/ml)*
–	–	16 ± 3
–	+	280 ± 25
+	–	13 ± 2
+	+	59 ± 10*

Cultured cells were pretreated with 30 μM minodronate or vehicle for 8 h, then stimulated by 0.1 μM TPA or vehicle for 48 h. Cell viability after treatment was more than 90% of control cells. Each value represents the mean ± SD of triplicate determinations. Similar results were obtained with two additional and different cell preparations. *$p < 0.05$ compared to the value of TPA alone.

thesis of VEGF (Table 1). Minodronate (30 μM) caused a reduction of approximately 80% in TPA effect (*$p < 0.05$, compared with the value of TPA alone).

Effects of minodronate on phosphorylation of MEK1/2 induced by PGF2α or TPA in MC3T3-E1 cells

Activation of p44/p42 MAP kinase is known to be regulated by MEK1/2 as a MAP kinase kinase, which is regulated by an upstream kinase known as Raf-1 [32]. We have previously found that $PGF_{2\alpha}$ or TPA stimulates phosphorylation of both MEK1/2 and Raf-1 in osteoblast-like MC3T3-E1 cells [22]. Thus, we next examined the effect of minodronate on phosphorylation of MEK1/2 induced by $PGF_{2\alpha}$. Minodronate, which alone did not affect phosphorylation of MEK1/2, significantly suppressed $PGF_{2\alpha}$ induced MEK1/2 phosphorylation (Fig. **2a**, *$p < 0.05$, compared with the value of $PGF_{2\alpha}$ alone). In addition, TPA-induced phos-

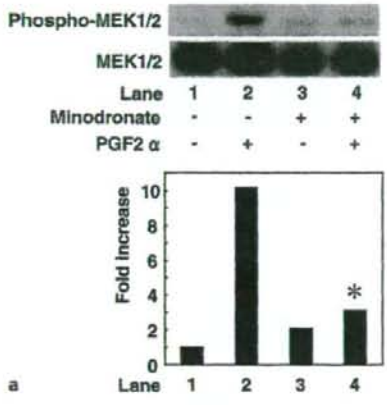

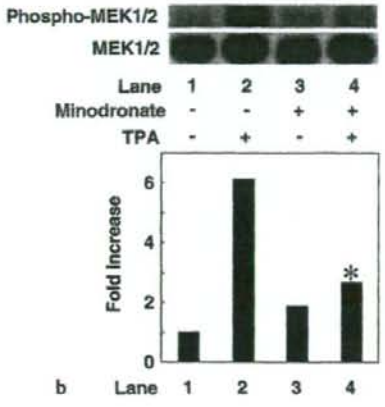

Fig. 2 Effects of minodronate on phosphorylation of MEK1/2 induced by PGF2α or TPA in MC3T3-E1 cells. (A) Cultured cells were pretreated with 10 μM minodronate or vehicle for 8 h, then stimulated by 10 μM $PGF_{2\alpha}$ or vehicle for 30 min. (B) The cultured cells were pretreated with 10 μM minodronate or vehicle for 8 h, then stimulated by 0.1 μM TPA or vehicle for 60 min. Extracts of cells were subjected to SDS-PAGE with subsequent Western blot analysis using antibodies against phosphospecific MEK1/2 or MEK1/2. The histogram shows quantitative representations of MEK1/2 phosphorylation obtained from laser densitometric analysis. Each value represents the mean of triplicate determinations. Similar results were obtained with two additional and different cell preparations. *$p < 0.05$, compared to the value of $PGF_{2\alpha}$ alone or TPA alone.

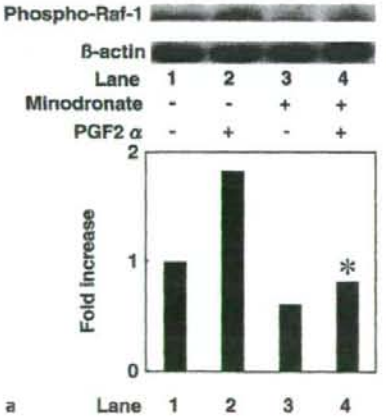

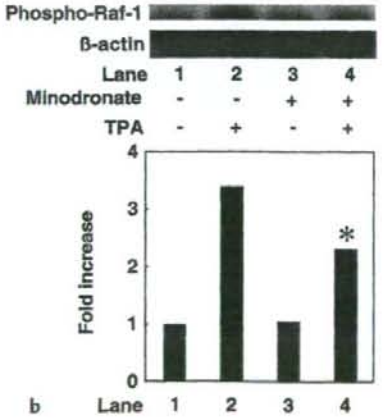

Fig. 3 Effects of minodronate on phosphorylation of Raf-1 induced by PGF2α or TPA in MC3T3-E1 cells. (**a**) The cultured cells were pretreated with 10 μM minodronate or vehicle for 8 h, then stimulated by 10 μM $PGF_{2\alpha}$ or vehicle for 15 min. (**b**) The cultured cells were pretreated with 10 μM minodronate or vehicle for 8 h, then stimulated by 0.1 μM TPA or vehicle for 60 min. Extracts of cells were subjected to SDS-PAGE with subsequent Western blot analysis using antibodies against phosphospecific Raf-1 or β-actin. The histogram shows quantitative representations of MEK1/2 phosphorylation obtained from laser densitometric analysis. Each value represents the mean of triplicate determinations. Similar results were obtained with two additional and different cell preparations. *$p < 0.05$ compared to the value of $PGF_{2\alpha}$ alone or TPA alone.

Table 2 Effect of mevalonate on minodronate inhibition of PGF2α-induced VEGF synthesis in osteoblast-like MC3T3-E1 cells

Minodronate	Mevalonate	PGF2α	VEGF (pg/ml)
–	–	–	33.0±4.4
–	–	+	1095.0±78.0
–	+	–	26.0±4.5
–	+	+	1188.0±282.1
+	–	–	16.0±3.4
+	–	+	94.7±4.2*
+	+	–	17.0±3.5
+	+	+	81.3±4.5*

Cultured cells were pretreated with 10 μM minodronate, 10 μM mevalonate or vehicle for 8 h, then stimulated by 10 μM $PGF_{2\alpha}$ or vehicle for 48 h. The cell viability after the treatments was more than 90% of control cells. Each value represents the mean ± SD of triplicate determinations. Similar results were obtained with two additional and different cell preparations. *$p < 0.05$, compared to the value of $PGF_{2\alpha}$ alone.

phorylation of MEK1/2 was markedly attenuated (Fig. **2b**, *$p < 0.05$, compared with the value of TPA alone).

Effects of minodronate on phosphorylation of Raf-1 induced by PGF2α or TPA in MC3T3-E1 cells

Previously, we reported that $PGF_{2\alpha}$ or TPA stimulated phosphorylation of Raf-1 in osteoblast-like MC3T3-E1 cells [22]. To clarify whether the effect of minodronate is exerted at a point upstream of Raf-1 or not, we examined the effect of minodronate on phosphorylation of Raf-1 induced by $PGF_{2\alpha}$ or TPA. Minodronate by itself did not affect Raf-1 phosphorylation, but significantly reduced phosphorylation of Raf-1 induced by $PGF_{2\alpha}$ (Fig. **3a**) or TPA (Fig. **3b**) (*$p < 0.05$, compared with the value of $PGF_{2\alpha}$ alone or TPA alone). According to densitometric analysis, minodronate (10 μM) caused a reduction of approximately 60% in the effect of $PGF_{2\alpha}$.

Effects of mevalonate on minodronate inhibition of PGF2α-induced VEGF synthesis in MC3T3-E1 cells

To clarify whether the mevalonate pathway is involved in minodronate inhibition of VEGF synthesis by $PGF_{2\alpha}$, we investigated the effect of mevalonate on the inhibition of VEGF synthesis by $PGF_{2\alpha}$ in MC3T3-E1 cells. Mevalonate, which alone had no effect on VEGF levels, did not affect either VEGF synthesis induced by $PGF_{2\alpha}$ or minodronate inhibition of $PGF_{2\alpha}$-induced VEGF synthesis (Table **2**).

Discussion

In contrast to the inhibitory effect of minodronate presented here, we have recently reported that incadronate, a nitrogen-containing bisphosphonate, but not alendronate enhances VEGF synthesis induced by $PGF_{2\alpha}$ in osteoblast-like MC3T3-E1 cells [22]. In contrast, we have recently reported that non-amino-bisphosphonate tiludronate, but not etidronate, inhibits $PGF_{2\alpha}$-induced VEGF release [23]. Thus, these findings suggest that the effects of bisphosphonates on $PGF_{2\alpha}$-induced VEGF synthesis in osteoblasts are compound-specific and vary among bisphosphonates. Pamidronate and zoledronate reportedly induce avascular necrosis of the jaw in a clinical setting [33,34], but no other bisphosphonates – including tiludronate and etidronate – are associated with avascular necrosis [33]. Taken together, the specific effects of each agent may be involved in clinical applications, supporting our present findings showing the agent-specific effects of bisphosphonates.

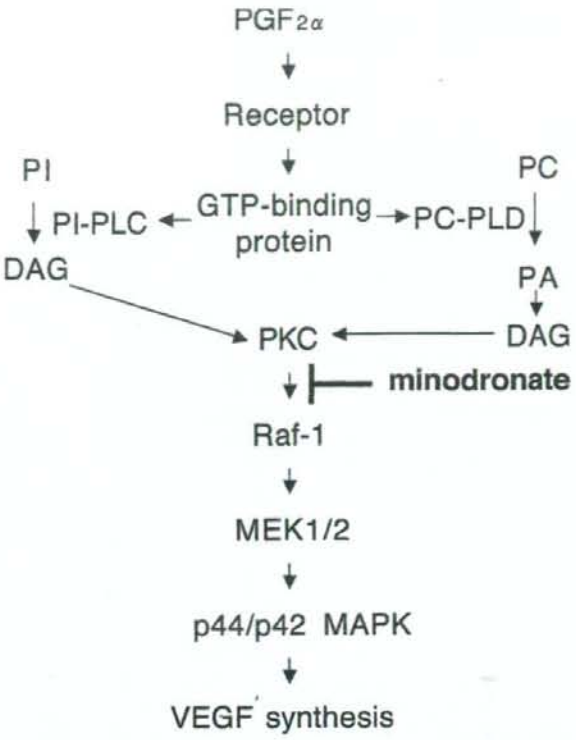

Fig. 4 Potential mechanisms in minodronate suppression of PGF2α-induced VEGF synthesis in MC3T3-E1 cells. GTP-binding protein, heterotrimeric GTP-binding protein; PI-PLC, phosphoinositide-hydrolyzing phospholipase C; PC-PLD, phosphatidylcholine-hydrolyzing phospholipase D,; PA, phosphatidic acid; DAG, diacylglycerol; PKC, protein kinase C; MAPK, mitogen-activated protein kinase; VEGF, vascular endothelial growth factor.

We previously reported that $PGF_{2\alpha}$ activated both PI-phospholipase C and PC-phospholipase D via heterotrimeric GTP-binding protein in osteoblast-like MC3T3-E1 cells [18,19], and also that $PGF_{2\alpha}$ activated p44/p42 MAP kinase in a PKC-dependent manner in these cells [35]. PI hydrolysis by phospholipase C and PC hydrolysis by phospholipase D are recognized as two major PKC-activating pathways [20,21]. In addition, we reported that $PGF_{2\alpha}$-induced VEGF synthesis through PKC-dependent, and probably PKCβI-dependent activation of p44/p42 MAP kinase in MC3T3-E1 cells [22]. Thus, we investigated the mechanism of minodronate underlying the inhibition of $PGF_{2\alpha}$-induced VEGF synthesis.

It is generally recognized that p44/p42 MAP kinase is activated through phosphorylation of threonine and tyrosine residues by dual-specificity MAP kinase kinase, known as MEK1/2 [32]. MEK1/2 is known to be activated by its own phosphorylation in-

duced by MAP kinase kinase kinase, Raf-1 [32]. We have demonstrated that minodronate also suppresses $PGF_{2\alpha}$ or TPA-induced phosphorylation of MEK1/2 and Raf-1. Taking our results as a whole, it is most likely that minodronate exerts its suppressive effect at the point between PKC and Raf-1 in $PGF_{2\alpha}$-stimulated VEGF synthesis in osteoblast-like MC3T3-E1 cells (Fig. **4**).

In the previous study, we reported that incadronate enhanced [22], while tiludronate suppressed [23] $PGF_{2\alpha}$-induced VEGF synthesis in MC3T3-E1 cells. Interestingly, the amplifying and suppressive effects of incadronate and tiludronate are exerted at a point between PKC and Raf-1 [22,23], where minodronate also showed suppressive effect in the present study. These findings suggest the different molecular mechanisms among the actions of bisphosphonates on osteoblasts, most likely their structural differences. There are considerable structural differences among these agents at the R2 side chain. Minodronate possesses 1-hydroxy-2-imidazo-(1, 2-a) pyridin-3-ylethylidene structure, and incadronate possess cycloheptylaminomethylene and 1-hydroxyethylidene structures [4], and tiludronate possesses (4-chlorophenyl) thiolmethylene structure with a more simple non-nitrogen-containing R2 side chain. In addition, the different effects of these bisphosphonates on VEGF synthesis may be related to their relative potency on anti-bone resorptive activities in these agents. In metabolic bone diseases, bone remodeling rates vary from case to case. To clarify the unique agent-specific effect(s) among bisphosphonates, it may be possible to select bisphosphonates according to the specific effect on bone-forming cells in adequate therapy by these drugs. Our present data together with our previous studies [22,23] would provide a new insight into the differences in pharmacological effects among bisphosphonates possibly due to their structural differences at the R2 side chain. Further investigation would be required to clarify the exact mechanism of bisphosphonate action on bone cells.

Nitrogen-containing bisphosphonates including minodronate are known to affect the mevalonate pathway and inhibit farnesyl diphosphate synthase [4]. We found that mevalonate did not affect the suppressive effect of minodronate on VEGF synthesis by $PGF_{2\alpha}$ in MC3T3-E1 cells. Therefore, it seems unlikely that mevalonate pathway is involved in the suppressive effect of minodronate on VEGF synthesis by $PGF_{2\alpha}$ in osteoblast-like MC3T3-E1 cells. In the present study, the effect of minodronate was significant at considerably higher doses than in clinical use. According to pharmacokinetic studies on bisphosphonates, these agents mainly accumulate in bone tissue *in vivo*[4]. Minodronate concentrations in the region probably reach much higher levels than do serum concentrations. Therefore, it is possible that the effect of minodronate shown here might be implicated in clinical relevance.

In conclusion, our present data strongly suggest that minodronate suppresses VEGF synthesis stimulated by $PGF_{2\alpha}$ in osteoblasts, and the inhibitory effect is exerted at the point between PKC and Raf-1.

Acknowledgments

This work was supported in part by a grant-in-aid for scientific research (16590873, 16591482) from the Ministry of Education, Science, Sports and Culture of Japan and research grants for longevity sciences (15A-1 and 15C-2) and health and labor sciences research grant for research on proteomics from the Ministry of Health, Labor and Welfare of Japan. The authors are very grateful to Mrs. S. Sakakibara for her skillful secretarial assistance.

References

[1] Nijweide PJ, Burger EH, Feyen JHM. Cells of bone: Proliferation, differentiation and hormonal regulation. Physiol Rev 1986; 66: 855–886
[2] Suda T, Takahashi N, Udagawa N, Jimi E, Gillespie MT, Martin TJ. Modulation of osteoclast differentiation and function by the new members of the tumor necrosis factor receptor and ligand families. Endocrine Rev 1999; 20: 345–357
[3] Erlebacher A, Filvaroff EH, Girelman SE, Derynck R. Toward a molecular understanding of skeletal development. Cell 1995; 80: 371–378
[4] Fleisch H, Reszka A, Rodan GA, Rogers M. Bisphosphonates. In: Bilezikian JP, Ratsz LG, Rodan GA (eds). Principles of Bone Biology 2nd Ed. San Diego, CA: Academic Press, 2002: 1361–1385
[5] Sahni M, Guenther HL, Fleisch H, Collin P, Martin TJ. Bisphosphonates act on rat bone resorption through the mediation of osteoblasts. J Clin Invest 1993; 91: 2004–2011
[6] Nishikawa M, Akatsu T, Katayama Y, Yasutomo Y, Kado S, Kugai N, Yamamoto M, Hagata N. Bisphosphonates act on osteoblastic cells and inhibit osteoclast formation in mouse marrow cultures. Bone 1995; 18: 9–14
[7] Vitte C, Fleisch H, Guenther HL. Bisphosphonates induce osteoblasts to secrete an inhibitor of osteoclast-mediated resorption. Endocrinology 1996; 137: 2324–2333
[8] Tokuda H, Kozawa O, Harada A, Uematsu T. Minodronate inhibits interleukin-6 synthesis in osteoblasts: Inhibition of phospholipase D activation in MC3T3-E1 cells. J Cell Biochem 1998; 69: 252–259
[9] Plotkin LI, Weinstein RS, Parfitt AM, Roberson PK, Manolagas SC, Bellido T. Prevention of osteocyte and osteoblast apoptosis by bisphosphonates and calcitonin. J Clin Invest 1999; 104: 1363–1374
[10] Reinholz GG, Getz B, Pederson L, Sanders ES, Subramaniam M, Ingle JN, Spelsberg TC. Bisphosphonates directly regulate cell proliferation, differentiation, and gene expression in human osteoblasts. Cancer Res 2000; 60: 6001–6007
[11] Viereck V, Emos G, Lauck V, Frosch KH, Blaschke S, Grundker C, Hofbauer LC. Bisphosphonates pamidronate and zoledronic acid stimulate osteoprotegerin production by primary human osteoblasts. Biochem Biophys Res Commun 2002; 291: 680–686
[12] Mackie PS, Fisher JL, Zhou H, Choong PF. Bisphosphonates regulate cell growth and gene expression in the UMR 106–01 clonal rat osteosarcoma cell line. Br J Cancer 2001; 84: 951–958
[13] Pan B, To LB, Farrugia AN, Findlay DM, Green J, Gronthos S, Evdokiou A, Lynch K, Atkins GJ, Zannettino ACW. The nitrogen-containing bisphosphonate, zoledronic acid, increases mineralization of human bone-derived cells in vitro. Bone 2004; 34: 112–123
[14] Pan B, Farrugia AN, To LB, Findlay DM, Green J, Lynch K, Zannettino ACW. The nitrogen-containing bisphosphonate, zoledronic acid, influences RANKL expression in human osteoblast-like cells by activating TNF-α converting enzyme (TACE). J Bone Miner Res 2004; 19: 147–154
[15] Ferrara N, Davis-Smyth T. The biology of vascular endothelial growth factor. Endocrine Rev 1997; 18: 4–25
[16] Gerber HP, Vu TH, Ryan AM, Kowalski J, Werb Z, Ferrara N. VEGF couples hypertrophic cartilage remodeling, ossification and angiogenesis during endochondral bone formation. Nat Med 1999; 5: 623–662
[17] Harada S, Thomas KA. Vascular endothelial growth factors. In: Bilezikian JP, Ratsz LG, Rodan GA (eds). Principles of Bone Biology 2nd Ed. San Diego, CA: Academic Press, 2002: 883–902
[18] Miwa M, Tokuda H, Tsushita K, Kotoyori J, Takahashi Y, Ozaki N, Kozawa O, Oiso Y. Involvement of pertussis toxin-sensitive GTP-binding protein in prostaglandin $F_{2\alpha}$-induced phosphoinositide hydrolysis in

osteoblast-like cells. Biochem Biophys Res Commun 1990; 171: 1229–1235
[19] Kozawa O, Suzuki A, Kotoyori J, Tokuda H, Watanabe Y, Ito Y, Oiso Y. 1994 Prostaglandin $F_{2\alpha}$ activates phospholipase D independently from activation of protein kinase C in osteoblast-like cells. J Cell Biochem 1994; 55: 373–379
[20] Nishizuka Y. Intracellular signaling by hydrolysis of phospholipids and activation of protein kinase C. Science 1992; 258: 607–614
[21] Exton JH. Regulation of phospholipase D. Biochim Biophys Acta 1999; 1439: 121–133
[22] Tokuda H, Harada A, Hirade K, Matsuno H, Ito H, Kato K, Oiso Y, Kozawa O. Incadronate amplifies prostaglandin $F_{2\alpha}$-induced vascular endothelial growth factor synthesis in osteoblasts. Enhancement of MAPK activity. J Biol Chem 2003; 278: 18930–18937
[23] Yoshida M, Tokuda H, Ishisaki A, Kanno Y, Harada A, Shimuzu K, Kozawa O. Tiludronate inhibits prostaglandin $F_{2\alpha}$-induced vascular endothelial growth factor synthesis in osteoblasts. Mol Cell Endocrinol 2005; 236: 59–66
[24] Sudo M, Kodama H, Amagai Y, Yamamoto S, Kasai S. In vitro differentiation and calcification in a new clonal osteogenic cell line derived from newborn mouse calvaria. J Cell Biol 1983; 96: 191–198
[25] Kanno Y, Ishisaki A, Yoshida M, Nakajima K, Tokuda H, Numata O, Kozawa O. Adenylyl cyclase-cAMP system inhibits thyroid hormone-stimulated osteocalcin synthesis in osteoblasts. Mol Cell Endocrinol 2005; 229: 75–82
[26] Noda T, Tokuda H, Yoshida M, Yasuda E, Hanai Y, Takai S, Kozawa O. Possible involvement of phosphatidylinositol 3-kinase/Akt pathway in insulin-like growth factor-I-induced alkaline phosphatase activity in osteoblasts. Horm Metab Res 2005; 37: 270–274
[27] Kozawa O, Suzuki A, Tokuda H, Uematsu T. Prostaglandin $F_{2\alpha}$ stimulates interleukin-6 synthesis via activation of PKC in osteoblast-like cells. Am J Physiol 1997; 272: E208–E211
[28] Laemmli UK. Cleavage of structural proteins during the assembly of the head of bacteriophage T4. Nature 1970; 227: 680–685
[29] Kato K, Ito K., Hasegawa K, Inaguma Y, Kozawa O, Asano T. Modulation of the stress-induced synthesis of hsp27 and αB-crystalin by cyclic AMP in C6 rat glioma cells. J Neurochem 1996; 66: 946–950
[30] Nishizuka Y. Studies and perspectives of protein kinase C. Science 1986; 233: 305–312
[31] Hatakeyama D, Kozawa O, Otsuka T, Shibata T, Uematsu T. Zinc suppresses IL-6 synthesis by prostaglandin F2α in osteoblasts: inhibition of phospholipase C and phospholipase D. J Cell Biochem 2002; 85: 621–628
[32] Widmann C, Gibson S, Jarpe MB, Johnson GL. Mitogen-activated protein kinase: conservation of a three-kinase module from yeast to human. Physiol Rev 1999; 79: 143–180
[33] Marx RE. Pamidronate (Aredia) and zoledronate (Zometa) induced avascular necrosis of the jaws: a growing epidemic. J Oral Maxillofac Surg 2003; 61: 1115–1118
[34] Carter GD, Goss AN. Bisphosphonates and avascular necrosis of the jaws. Aust Dent J 2003; 48: 268
[35] Tokuda H, Kozawa O, Harada A, Uematsu T. p42/p44 mitogen-activated protein kinase activation is involved in prostaglandin $F_{2\alpha}$-induced interleukin-6 synthesis in osteoblasts. Cell Signal 1999; 11: 325–330

1．大腿骨頸部骨折

大腿骨頸部骨折は重篤度と頻度からみて最大の骨粗鬆症合併症であり，それによる生命，機能，生活の質（QOL：quality of life）損失には大きなものがあり，その医療と介護には莫大な費用が必要である。それらの医療経済的評価には，死亡だけでなく，生存期間のQOLが重要で，治療法の正しい評価にもQOLで補正された生存年あたりの費用が必要である[1]。その参考となるべく，ここでは大腿骨頸部骨折の予後とQOLについて記述する。

大腿骨頸部骨折の合併症

1）急性期合併症

入院中合併症の発生率は，米国における大腿骨頸部骨折患者510名の研究によれば43%で，頻度順に電解質バランス不良(11%)，尿路感染（10%），呼吸器系障害（10%），譫妄（9%）であった[2]。わが国でもほとんど同じ率が報告されており，大腿骨頸部骨折525例において術後の合併症は44%に生じて，譫妄が9.3%，循環器疾患4.4%，肺炎が3.2%であった[3]。日本整形外科学会による大腿骨頸部/転子部骨折診療ガイドラインによれば，日本の多くの報告から，わが国の術後合併症は，肺炎が最も多く，次いで心不全としている[4]。性別では，別の983例の調査で，男性は，術後合併症発生率が21.4%と女性の13.8%より高く，術後合併症の危険因子となっていた[5]。合併症による入院中死亡率は，日本整形外科学会の骨粗鬆症委員会による1999年より2001年発生分の定点観測によると，3年間で集められた12,250例のうち，409名が入院中死亡し3.3%であった[6]。入院中死亡の原因はやはり肺炎が30～44%で最も多い[4]。ちなみに譫妄は，12研究1,823例によるシステマティックレビューでは，頻度は35%と高く，その危険因子は老齢と認知症だけであった[7]。

2）慢性期合併症

骨折そのものに由来する合併症としては偽関節があり，その発生率は，大腿骨頸部内側骨折の非転位型で0～15%，転位型では4～40%とされ，大腿骨転子部骨折では0.8～2.9%とされる[4]。また，大腿骨頸部内側骨折後の骨頭壊死で骨頭陥没にいたる率は，非転位型で0～8%，転位型で26～41%とされる[4]。さらに，人工骨頭施行後には22.4%に異所性骨化が発生しており，骨化が重症の例では歩行能力が低下するとされる[8]。

全身合併症は，高齢で脆弱な患者が多いため様々な疾患が起こりうるが，死因となる合併症としては，肺炎[9~12]，心不全[9~11]，脳血管障害[9,10]，悪性腫瘍[12]などが主なものである。しかし，大谷のロジスティック解析では，これらの合併症の退院後死亡への関連性は消失し，退院時歩行不能だけがオッズ比5.4の危険因子として残ったとされ[13]，機能予後と生命予後が密接に関連していることがうかがえる。

大腿骨頸部骨折の予後

1）生命予後

骨粗鬆症による骨折の中で，大腿骨頸部骨折は前述したような合併症発生も多く，生命予後に最も影響する。デンマークのJensenらは1979年に大腿骨頸部骨折患者1,592例を調査して，骨折後死亡率が3カ月で17%，6カ月で22%，1年で27%，5年で56%と，骨折後の生存曲線が骨折後1.6年までは期待生存曲線より急峻に低下し，その後は期待生存曲線と平行に推移するとしている[14]。どの年代でも大腿骨頸部骨折直後は死亡率が一般住民より上昇し，それ以後6カ月以降まで下降するが，その後も一般住民より高率にとどまる[15]というパターンは時代と国を越えて共通のものと考えられる。ただし，その内容は社会情勢に左右されて異なっており，死亡率は北欧，日本では時代とともに改善しているが，英国ではあまり変わらず[16]，2005年に英国のRocheらが大腿骨頸部骨折2,090例を前向き調査した報告をみても，骨折後死亡率は術後30日で9.6%，1年で33%と相変わらず高いレベルにとどまっている[17]。

わが国では，七田らの1988年の研究が最初で，1,048例中867例を追跡し，死亡率は6カ月で8%，1年で14%，2年で35%と報告